ELSEVIER

Catalysis Today 48 (1999) 57–63

CATALYSIS TODAY

Modelling of citral hydrogenation kinetics on an Ni/Al_2O_3 catalyst

Lasse-Pekka Tiainen*, Päivi Mäki-Arvela, Tapio Salmi

Laboratory of Industrial Chemistry, Åbo Akademi, Turku, Finland

Abstract

The kinetics of citral hydrogenation in ethanol over an Ni/Al_2O_3 catalyst was studied in a slurry reactor operating at atmospheric pressure and at a temperature range of 60–77°C. Citronellal was the primary reaction product, whereas the amounts of unsaturated alcohols were very minor. Citronellol was the dominating product, generated mainly through the hydrogenation of the carbonyl group of citronellal. Based on the experimental data, a kinetic model was developed for hydrogenation. The model comprises competitive and rapid adsorption steps as well as rate-determining hydrogenation steps. The mass transfer limitation of hydrogen was included in the mathematical model. The kinetic parameters and the mass transfer parameter of hydrogen were estimated from the experimental data. A comparison of the model predictions with the experimental data revealed that the proposed kinetic approach gave a satisfactory reproduction of the data.

Keywords: Citral hydrogenation; Kinetics; Ni/Al_2O_3 catalyst

1. Introduction

Citral is an interesting model compound for hydrogenation, since it contains both an isolated and a conjugated double bond as well as a carbonyl group, and it exists as cis and trans isomers. In citral hydrogenation, the most important product is citronellol, which is used e.g. in perfumery industry [1]. The primary hydrogenation product is citronellal, which reacts further to citronellol and 3,7-dimethyloctanol. There also exist other products formed in this system, namely the unsaturated alcohols (nerol and geraniol). When citral is hydrogenated in ethanol, citronellal acetals can be formed. The stoichiometric scheme of citral hydrogenation in alcohol solvents is shown below:

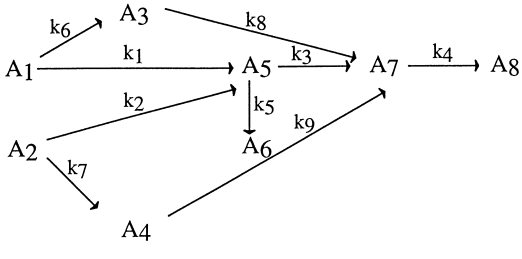

where: A_1=*cis*-citral, A_2=*trans*-citral, A_3=nerol, A_4=geraniol, A_5=citronellal, A_6=acetal of citronellal, A_7=citronellol and A_8=3,7-dimethyloctanol.

In the present work, we consider the modelling of citral hydrogenation kinetics in a batch reactor, under the influence of the mass transfer resistance of hydrogen.

*Corresponding author.

0920-5861/99/$ – see front matter
PII: S0920-5861(98)00358-7

2. Experimental

The hydrogenation experiments were carried out at atmospheric pressure in a five-necked 100 ml glass reactor equipped with a magnetic stirring bar and an electrical heater with a temperature controller and thermocouples. Hydrogen (99.999%, AGA) was dispersed into the reaction mixture through separate glass sinters. The desired amount of catalyst, Ni/Al_2O_3 (16.7 wt% Ni, Crosfield, HTC-400) was transferred into the reactor and activated under hydrogen flow under dry conditions and then dispersed in ethanol. The desired amount of citral was injected into the reactor and the hydrogenation was commenced. Samples were withdrawn for analysis. The samples were analysed with a gas chromatograph equipped with a capillary column and an FI detector. Temperature programming was applied.

The solubility of hydrogen in ethanol at the experimental temperatures was metered with a gas chromatograph equipped with a packed column and a TC detector. The catalyst was characterized with temperature programmed desorption, hydrogen chemisorption, X-ray diffraction and nitrogen physisorption.

3. Results and discussion

3.1. Catalyst characterization

According to the chemisorption measurements, the metal dispersion was 15.4%. XRD and chemisorption measurements were in good agreement giving an average metal particle size of about 66 Å.

3.2. Mass transfer effects in kinetics

Preliminary experiments were carried out with different hydrogen flows and catalyst particle sizes to check whether the reaction conditions were beyond external and internal mass transfer limitations. The roles of external and internal mass transfer resistances were investigated with three different kinds of experiments: hydrogenation with different flow rates, hydrogenation with different particle sizes and, finally, hydrogenation with different amounts of catalyst.

The catalyst was reduced at 350°C for 2 h prior to the experiment. Citral was hydrogenated at 70°C with two different hydrogen flows: 75 and 100 ml/min. With these hydrogen flows, no considerable differences in the yields of different products could be detected, i.e. it can be assumed that hydrogen concentration in the liquid phase was virtually constant. Two different particle sizes were tested in hydrogenation: <45 and 65–90 μm. No significant differences were found in the hydrogenation velocities. In all other experiments, a hydrogen flow of 100 ml/min and particle sizes of 63–90 μm were used.

In the semibatch reactor, the yields of different compounds should be equal with different amounts of the catalyst as a function of the catalyst mass multiplied by the reaction time and divided with the liquid volume, if the mass transfer effects are absent. However, the yields of the compounds were not equal in comparable experiments. With the larger amount of the catalyst (the citral-to-nickel ratio 25), the yield of citronellol was lower than with a smaller amount of catalyst (the citral-to-nickel ratio 51). The same trend was obtained with a used catalyst with three different citral-to-nickel ratios, the yield of citronellol decreased in the order 100>51>25. The results indicate that there must be a lack of hydrogen on the catalyst surface with the larger catalyst amounts, i.e. the external mass transport of H_2 affected the hydrogenation process. The systematic kinetic experiments were carried out with the citral-to-nickel ratio of 25 and the mass transfer effect was included in the kinetic modelling.

3.3. Product distribution in kinetic experiments

A typical citral hydrogenation curve is shown in Fig. 1. The catalyst had been previously used in hydrogenation experiments. The reaction temperature was 70°C and the citral-to-Ni ratio was 25. The initial concentration of citral was 0.1 M. Citral reacted completely within the first 30 min and the yield of citronellal and its ethylacetal also attained the maximum level with about 30 min. Nerol and geraniol yields obtained their maxima at about 30 min. The yield of citronellol was at its maximum between 420 and 540 min, and it remained quite high for a long time. The formation of 3,7-dimethyloctanol became clearly visible after about 360 min. In the long-time experiment with Ni/Al_2O_3, the yield of citronellol remained rather stable during 3 h, after which it was hydroge-

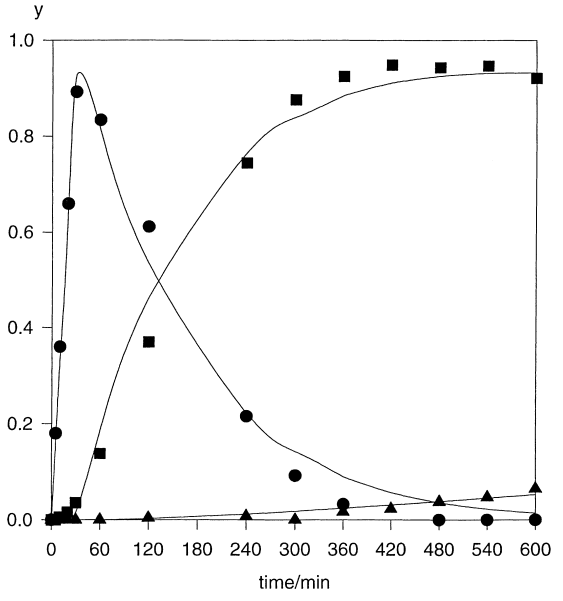

Fig. 1. The yields of citronellal (●), citronellol (■) and 3,7-dimethyloctanol (▲) at 70°C with 0.1 mol/l initial concentration of citral. Citral-to-Ni ratio=25.

nated further to 3,7-dimethyloctanol. With this catalyst, just small amounts of citronellal acetal were formed.

3.4. Concentration and temperature effects

The concentration effect of citral on the hydrogenation velocity was examined with five different citral concentrations using a catalyst, which had been preactivated at 500°C for 2 h and prior to the experiment at 350°C for 2 h. The optimum initial citral concentration was 0.05 M, for which the hydrogenation rate was highest. With the initial concentration of 0.3 M, the rate was slowest and for this slowest hydrogenation rate the acetal formation was largest. The observed concentration effect indicates that the adsorption of hydrogen and citral is of competitive character.

The influence of the temperature on the hydrogenation kinetics was studied at 60°C, 70°C and 77°C. A used catalyst was reduced at 350°C for 2 h before the experiment. The yield of citronellal attained its maximum fastest, after 30 min, at the lowest temperature, 60°C (Fig. 2). The yield of citronellol reached its maximum at 70°C (Fig. 2); at higher temperatures

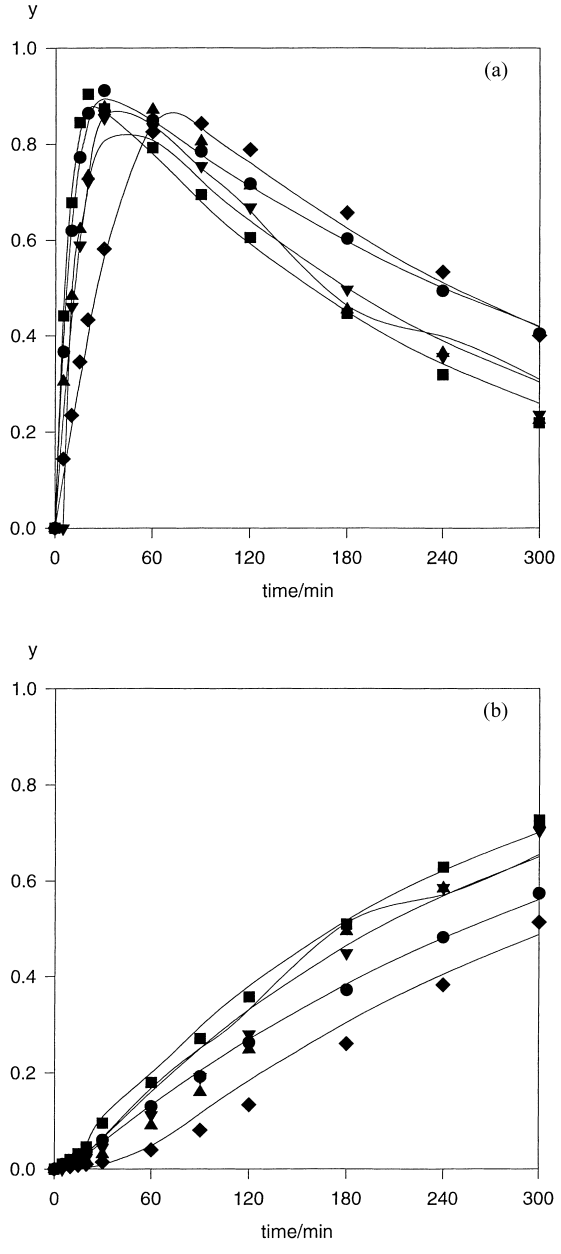

Fig. 2. The yields of citronellal (a) and citronellol (b) in citral hydrogenation with five different initial concentrations of citral. Conditions: citral-to-Ni ratio=25, 70°C. Symbols: initial concentrations of citral: 0.025 (●), 0.05 (■), 0.1 (▲), 0.2 (▼) and 0.3 M (◆).

the yield of citronellol was lower. The yields of nerol and geraniol also reached their maxima fastest at the lowest temperature, 60°C, and their amounts decreased with time, since they were hydrogenated

further to citronellol. The formation of citronellal acetal was slightly catalysed by the temperature increase, but the amounts of the acetals were about 1 mol% for the used catalyst.

When citral was hydrogenated over a catalyst which was preactivated at 500°C for 2 h and then before the experiment at 350°C for 2 h, the yield of citronellol decreased after 300 min in the following order: 77°C>70°C>60°C. This catalyst was less reduced than a used catalyst. The effect is also visible in the citronellal acetal formation, which was at 77°C about 6 mol% and even minor amounts of citral acetals were detected (confirmed with GC–MS); citral acetals were not at all found in the reaction mixture with a used catalyst (reduced at 350°C). When the catalyst was reduced at 500°C for 2 h, the reaction rate was slower than with a used catalyst. This was confirmed from TPD and chemisorption: the total amount of hydrogen desorbed from the catalyst reduced at a higher temperature is smaller than that from the catalyst reduced at a lower temperature. The amount of spillover hydrogen was larger for the catalyst preactivated at 500°C, but the amount of hydrogen desorbed from nickel was smaller than for the used catalyst [2]. This can be explained by the catalyst sintering, which starts with the catalyst preactivated at 500°C at temperatures exceeding 424°C, as water commences to irreversibly desorb from the catalyst surface in the TPD experiment. This water is probably originated from the dehydroxylation of alumina support [3]. According to [4], the sintering of Ni metal begins at 450°C. Sintering did not diminish the catalyst surface area in our experiments. Since citral has a weaker adsorption on the fresh catalyst than on the used catalyst, more acetal can be formed on the fresh catalyst. The general conclusion from these experiments is that the chemical state of catalyst is of crucial importance in citral hydrogenation.

3.5. Kinetics and mechanism

The observed concentration effects suggest that the adsorption of the organic species, particularly citral, and hydrogen is of competitive nature. It is, however, possible that citral is not able to completely compete away all the hydrogen from the catalyst surface, because the much smaller hydrogen atoms might adsorb on interstitial sites remaining unoccupied by citral. In the modelling of the kinetics, the following mechanistic assumptions were made: the adsorption of hydrogen and the organic species is rapid, whereas the surface hydrogenation steps are rate determining. Hydrogen adsorption can in principle be dissociative or non-dissociative, but hydrogen is presumed to preserve its molecular identity during the hydrogenation, i.e. even in case of dissociative adsorption, two hydrogen atoms are simultaneously added to the double bond of the organic species. The hydrogenation steps are assumed to be irreversible, and the product desorption steps were presumed to be rapid. Based on these hypotheses, the reaction steps can be sketched as follows.

Adsorption steps:

$H_2 + \gamma^* \rightleftarrows \gamma H^*_{2/\gamma}$, where $\gamma=1$ or $\gamma=2$
$A_1 + * \rightleftarrows A_1^*$
$A_2 + * \rightleftarrows A_2^*$

Hydrogenation steps (the step number in the reaction scheme is given in brackets):

$A_1^* + \gamma H^*_{2/\gamma} \rightleftarrows A_3^* + \gamma^*$ [6]
$A_2^* + \gamma H^*_{2/\gamma} \rightleftarrows A_4^* + \gamma^*$ [7]
$A_1^* + \gamma H^*_{2/\gamma} \rightleftarrows A_5^* + \gamma^*$ [1]
$A_2^* + \gamma H^*_{2/\gamma} \rightleftarrows A_5^* + \gamma^*$ [2]
$A_5^* + \gamma H^*_{2/\gamma} \rightleftarrows A_7^* + \gamma^*$ [3]
$A_3^* + \gamma H^*_{2/\gamma} \rightleftarrows A_7^* + \gamma^*$ [8]
$A_4^* + \gamma H^*_{2/\gamma} \rightleftarrows A_7^* + \gamma^*$ [9]
$A_7^* + \gamma H^*_{2/\gamma} \rightleftarrows A_8^* + \gamma^*$ [4]

Acetalization steps:

$A_5 + 2ROH \rightleftarrows A_6^*$ [5]

Desorption steps:

$A_i^* \rightleftarrows A_i + *$, where $i=3,\ldots,8$

The rate of a hydrogenation step can thus be written as

$$R_k = k_k \theta_{Aj} \theta_H^{\gamma}, \quad k = 1, \ldots, 9, \tag{1}$$

where k and j denote the indices of the reaction step and the organic compound taking part in the step. The surface coverages of the organic components and hydrogen are expressed with the adsorption–desorption quasi-equilibria: $K_{Aj}=\theta_{Aj}/(c_{Aj}\theta_\nu)$ and $K_H = \theta_H^{\gamma}/c_H\theta_\nu^{\gamma}$, where θ_ν is the fraction of vacant sites on the surface. The fractional coverages are solved from K_{Aj} and K_H and inserted in the rate expression

(1), which becomes

$$R_k = k_k K_{Aj} K_H c_{Aj} c_H \theta_\nu^{\gamma+1}. \quad (2)$$

The fractional coverages are coupled via the site balance ($\sum\theta_{Al}+\theta_H+\theta_\nu=1$), the quasi-equilibrium expressions K_{Aj} and K_{Hj} are inserted in the site balance, and the fraction of vacant sites is solved and inserted in the rate expression, which becomes

$$R_k = k_k K_{Aj} K_H c_{Aj} \frac{c_H}{\left(1 + (K_H c_H)^{1/\gamma} + \sum K_{Al} c_{Al}\right)^{\gamma+1}}. \quad (3)$$

Eq. (3) implies that the order of the denominator can vary between 2 and 3, corresponding to non-dissociative and dissociative adsorption, respectively. Independent hydrogen adsorption measurements [5] suggest, however, that dissociative adsorption might be the most probable state for nickel. According to the model, the overall reaction orders with respect to the organic species and hydrogen are ≤ 1. In practice it turned out that it was possible to ignore the terms in the denominator of Eq. (3), since the component concentrations were low.

3.6. Reactor model

The hydrogenation reactor is described quantitatively according to the following principles: the liquid phase is in batch, whereas pure hydrogen is continuously bubbled through the liquid phase; the gas–liquid–solid mass transfer resistance of hydrogen is included in the model, but the pseudo-steady state hypothesis is assumed to be valid for dissolved hydrogen. The liquid volume was approximated to be constant, since the liquid phase was strongly dominated by the solvent. Consequently, the model of the isothermal (semi)mass reactor becomes

$$\frac{dc_i}{dt} = \rho_B r_i = \rho_B \sum \nu_{ik} R_k, \quad (4)$$

where the catalyst bulk density is $\rho_B = m_{cat}/V_L$.

For dissolved hydrogen, the mass balance is written as follows:

$$N_{GLH} A_{GL} = N_{LSH} A_{LS} + dn_H/dt, \quad (5)$$

where N_{GLH} and N_{LSH} denote the fluxes at the gas–liquid and liquid–solid interphases, respectively. The pseudo-steady state hypothesis implies that $dn_H/dt = 0$. The interfacial fluxes were defined with simple expressions based on the film theory and Fick's law.

For the catalyst particle and the liquid film surrounding the particle, the hydrogen mass balance becomes

$$N_{LSH} A_{LS} + r_H m_{cat} = 0, \quad (6)$$

where the consumption rate of hydrogen is calculated from the reaction rates

$$r_H = \frac{-|\nu_H| \sum k_k K_H K_{Aj} c_{Aj} c_H}{D^{\gamma+1}} = -f c_H. \quad (7)$$

After inserting flux expressions in balance Eqs. (5) and (6) we can write the hydrogen concentration in an implicit form

$$c_H = \frac{c_H^*}{1 + m_{cat} f/(K' V_L)}, \quad (8)$$

where c_H^* is the saturation concentration calculated from the hydrogen solubility in ethanol, K' is the gas–liquid–solid overall mass transfer parameter involving the mass transfer coefficients (k_G,k_L) and the interfacial area-to-volume ratios (a,a_S): $K'^{-1} = (k_{GLH} a)^{-1} + (k_{LSH} a_S)^{-1}$ and de facto an iterative solution of Eq. (8) is inevitable, since the concentration of dissolved hydrogen (c_H) on the catalyst surface is included in factor f, in the adsorption term (D). The saturation concentration of hydrogen was obtained from Henry's constant, calculated from hydrogen solubility data.

3.7. Parameter estimation and conclusions

Non-linear regression analysis was applied to the estimation of the rate and mass transfer parameters from experimental data. Stiff differential equation algorithms, a fourth order semi-implicit Rosenbrock–Wanner method (ROW4A) [6] was used for the numerical solution of the model equations and the Levenberg–Marquardt method [7] was applied to the minimization of the residual sum of squares. The following residual sum of squares was minimized:

$$Q = \sum (c_{i,t} - c'_{i,t})^2, \quad (9)$$

where i and t denote the organic compound and the experimental time, respectively. The prime in c

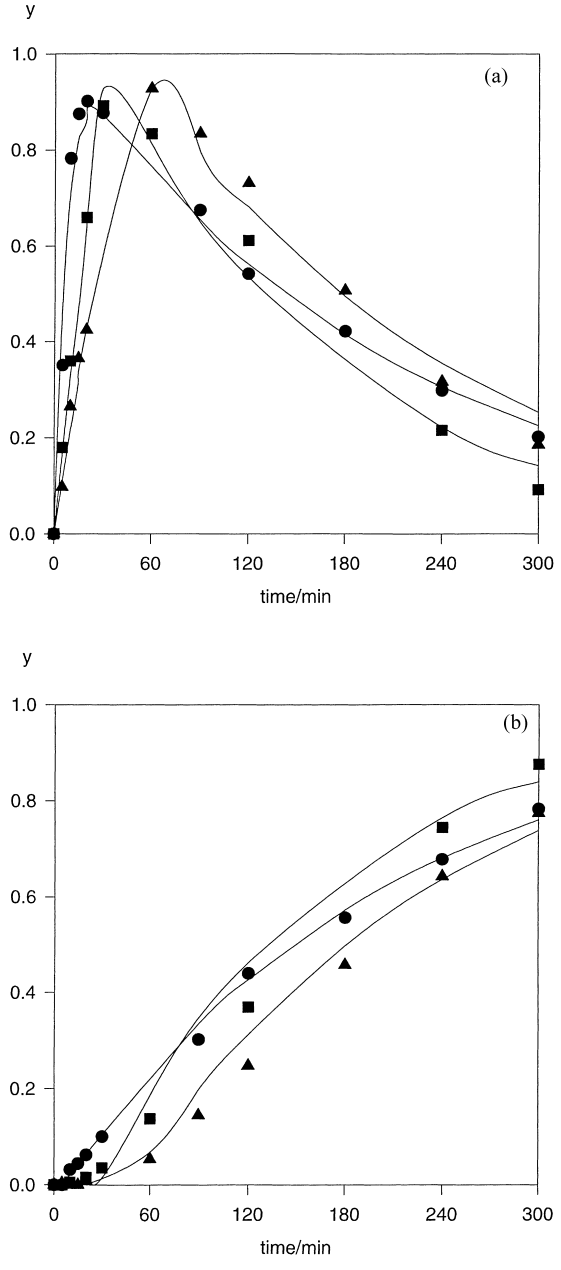

Fig. 3. The yields of citronellal (a) and citronellol (b) at temperatures 60°C (●), 70°C (■) and 77°C (▲). Conditions: the initial concentration of citral=0.1 M, citral-to-Ni ratio=25.

indicates the concentration predicted by the model, i.e. Eq. (4).

The hydrogen concentration was solved iteratively from Eq. (8) with one-dimensional Newton–Raphson method during the course of parameter estimation. The model equations were implemented in the software packages Reproche [8], which has in-built differential equation solvers and parameter estimation results.

The mass transfer parameter of hydrogen (K') was estimated together with the kinetic parameters. It turned out that the effect of the adsorption parameters could be ignored because of low concentrations.

The fit of the kinetic model is illustrated in Figs. 1–3. The kinetic parameters were rather well-identified and their mutual correlations are within reasonable limits.

The fit of the model shows that the model faithfully follows the experimental trends, the generation rates of the compounds as well as their mutual distribution. No larger deviations could be observed. The inflexion point of the kinetic curve of citronellol was not predicted very well; the reason might be that the desorption rate of citronellol contributes to the rate of the overall process. The incorporation of this effect in the kinetic model would, however, increase the number of adjustable parameters, which is unrealistic from the viewpoint of available kinetic data: the increase of the number of rate and equilibrium constants would lead to a very poor identifiability of the parameters. Thus we conclude that the proposed mathematical is sufficient for the description of the experimentally observed kinetics. In order to reveal the role of hydrogen in the kinetic behaviour, kinetic experiments under pressurized conditions are necessary.

Acknowledgements

The authors are grateful to Dr. Ensio Laine (University of Turku) for the XRD measurements, to Mr. Markku Reunanen for his contribution to the GC–MS analyses and to Dr. Johan Wärnå for his help in the parameter estimation.

References

[1] G. Neri, L. Mercadante, A. Donato, A. Visco, S. Galvagno, Catal. Lett. 29 (1994) 379.
[2] W. Conner, G. Pajonk, S. Teichner, Adv. Catal. 34 (1986) 1.

[3] J. Miller, B. Meyers, F. Modica, G. Lane, M. Vaarkamp, D. Koningsberger, J. Catal. 143 (1993) 395.
[4] P. Bolt, F. Habraken, J. Gens, J. Catal. 151 (1995) 300.
[5] P.W.J. Selwood (Ed.), Adsorption and Collective Paramagnetism, Academic Press, New York, 1962.
[6] P. Kaps, G. Wanner, Num. Math. 38 (1981) 279.
[7] D.W. Marquardt, J. Soc. Ind. Appl. Math. 11 (1963) 431.
[8] S. Vajda, P. Valkó, Reproche, Regression Program for Chemical Engineers, Eurecha, Budapest, 1985.